THE EUROPEAN
PHYSICAL JOURNAL C

Check for updates

Neutrino phenomenology and dark matter in an A_4 flavour extended $B − L$ model

Subhasmita Mishra[1,a], **Mitesh Kumar Behera**[2,b], **Rukmani Mohanta**[2,c], **Sudhanwa Patra**[3,d], **Shivaramakrishna Singirala**[4,e]

[1] Department of Physics, IIT Hyderabad, Kandi 502285, India
[2] School of Physics, University of Hyderabad, Hyderabad 500046, India
[3] Indian Institute of Technology Bhilai, GEC Campus, Sejbahar, Raipur 492015, India
[4] Discipline of Physics, Indian Institute of Technology Indore, Indore 453 552, India

Abstract We present an A_4 flavor extended $B − L$ model for realization of eV scale sterile neutrinos, motivated by the recent experimental hints from both particle physics and cosmology. The framework considered here is a gauged $B − L$ extension of standard model without the introduction of right-handed neutrinos, where the gauge triangle anomalies are canceled with the inclusion of three exotic neutral fermions N_i $(i = 1, 2, 3)$ with $B − L$ charges $− 4, − 4$ and 5. The usual Dirac Yukawa couplings between the SM neutrinos and the exotic fermions are absent and thus, the model allows natural realization of eV scale sterile-like neutrino and its mixing with standard model neutrinos by invoking A_4 flavor symmetry. We demonstrate how the exact tri-bimaximal mixing pattern is perturbed due to active-sterile mixing by analyzing $1 + 3$ case in detail. We also show the implication of eV scale sterile-like neutrino on various observables in neutrino oscillation experiments and the effective mass in neutrinoless double beta decay. Another interesting feature of the model is that one of three exotic fermions is required to explain eV scale phenomena, while other two fermions form stable dark matter candidates and their total relic density satisfy the observed 3σ limit of Planck data. We constrain the gauge parameters associated with $U(1)$ gauge extension, using relic density and collider bounds.

1 Introduction

Albeit its success, Standard Model (SM) is not the complete theory of nature to explain many observed phenomena. Neutrino oscillation experiments, in contrast to the zero mass prediction of SM, have confirmed the need for massive neutrinos and thus, necessitates for physics beyond the SM (BSM). The massive neutrinos and most of neutrino oscillation data can be explained in a framework of three active neutrinos through the elegant canonical seesaw mechanism [1–6], whereas some experimental observations are strongly hinting towards one or two additional light neutrinos with eV scale masses and $\mathcal{O}(0.1)$ mixing with active neutrinos [7–13], stemming from particle physics, cosmology and astrophysics (for details, reader may refer to the white paper [14]). While large number of experiments are coming up in next few years in order to investigate the possible presence of eV scale sterile neutrinos, which would be a ground-breaking discovery, there are few model building efforts in this direction. The aim of this work is to provide a simple BSM framework explaining the presence of one eV scale sterile neutrino along with $\mathcal{O}(0.1)$ mixing with active neutrinos and their effects on neutrinoless double beta decay (NDBD). This model also provides a detailed study of DM phenomenology via a TeV scale fermionic DM and the collider constraints from Z' mass.

The smallness of neutrino mass and their hierarchical structure become one of the most challenging problems in particle physics. In the standard scenario of three active neutrinos oscillation, two mass-squared differences of order 10^{-5} eV^2 and 10^{-3} eV^2, are observed from solar and atmospheric neutrino oscillation experiments respectively [15]. In fact, the absolute scale of neutrino mass still remains an open question to be solved, however, there exists an upper bound on the sum of active neutrino masses, $\sum m_\nu < 0.12$ eV from

[a] e-mail: subhasmita.mishra92@gmail.com

[b] e-mail: miteshbehera1304@gmail.com

[c] e-mail: rmsp@uohyd.ac.in (corresponding author)

[d] e-mail: sudhanwa@iitbhilai.ac.in

[e] e-mail: krishnas542@gmail.com

Springer

cosmological observations [16]. Over the last two decades, several dedicated experiments have determined the neutrino oscillation parameters rather precisely, though few of them are still unknown. These include the neutrino mass ordering, the exact domain of the atmospheric mixing angle θ_{23} (octant problem) and the CP violating phase δ_{CP}. But there exist few experimental anomalies, which can not be explained within the standard three neutrino framework. Of them, one is the possible presence of sterile neutrinos [17], which is evident from the anti-neutrino flux measurement in LSND [14] and MiniBooNE [18] experiments. The excess flux of $\bar{\nu}_e$ in appearance mode during $\nu_\mu \rightarrow \nu_e$ oscillation, hints towards the possible existence of at least one additional state with eV scale mass [19]. This new state should not have any gauge interaction as per the Z-boson precision measurement and hence being sterile in nature. Thus, theoretical explanation of eV scale sterile neutrinos and its order of 0.1 mixing with the active neutrinos is worth to study through possible BSM frameworks. The non-trivial mixing of such a light sterile neutrino with SM neutrinos are well studied in the literature within different seesaw framework [20–30]. Though there seems to be a tension between the cosmological observation and neutrino oscillation results from short baseline experiments regarding the existence of eV scale sterile neutrino, which is quite incompatible with the cosmologically observed value of N_{eff}, there exist literature, where different solutions to these issues are discussed [31–36]. However, in our model we are not discussing a detailed study of N_{eff}, well keeping it as an interesting scope for the follow up work of the current model.Along with these issues, the nature of neutrinos, i.e., whether it is Dirac or Majorana also remains unexplained. The only way to test the Majorana nature of neutrinos is through the extremely rare lepton-number violating neutrino-less double beta decay (NDBD) experiments.

One more well-known challenging problem in particle cosmology is that, SM doesn't have any explanation about the existence of DM even though we have enough indirect gravitational evidence about its existence. Attempts have been made through DM getting scattered off the SM particles i.e., in the context of direct searches, and the well known collaborations include LUX, XENON, PICO, PandaX etc [37,38]. Study of excess in positron, electron or Gamma rays i.e., indirect signals, and the experiments include AMS-02, H.E.S.S, MAGIC, Fermi-LAT etc [39–43]. Apart from these, dark sector particle production is also probed in the accelerator experiments as well.

To explain these experimental discrepancies, SM needs to be extended with extra symmetries or particles. Discrete symmetries are mostly preferred by the phenomenologists for model building purpose as they restrict the interaction terms by giving a specific structure to the mass matrix. A_4 flavor symmetry is widely used in neutrino phenomenology as it gives the simple tribimaximal (TBM) mixing, which is more

or less compatible with the standard neutrino mixing matrix (U_{PMNS}). But this mixing pattern predicts a vanishing reactor mixing angle θ_{13} [44], which conflicts the current experimental observation. To address this issue various ways are preferred to perturb the TBM structure by adding minimal number of flavon fields and myriad amount of literature is focused on neutrino phenomenology with A_4 symmetry in the frameworks of different seesaw mechanism [44–50]. Apart from neutrino phenomenology, phenomenological study of DM has been made within A_4 framework [51–55], but very few literature have been devoted to study these phenomena with gauge extended A_4 flavor symmetric model. We consider a minimal extension of SM with A_4 and $U(1)_{B-L}$ symmetry in addition to three flavon fields and three singlet scalars, responsible for the breaking of A_4 and $U(1)_{B-L}$ symmetry respectively. This model includes three additional fermions with exotic $B-L$ charges of $-4, -4, 5$ to protect from triangle gauge anomalies. This extension enhances the predictability of the model by explaining different phenomenological consequences like DM, neutrino mass and NDBD, compatible with the current observations. The minimal $B-L$ gauge extension of Standard Model with one copy of right-handed neutino having $B-L$ charge as -1 per generation or popular left-right theories [56–60] (where $B-L$ charge has a physical meaning with electric charge) provides an easier platform to explain the light neutrino masses through seesaw mechanism as well as the baryon asymmetry of the universe through leptogenesis. However, these theories fail to accomodate a stable cold dark matter candidate without imposition of ad-hoc discrete symmetry or inclusion of additional particles (see a recent work [61] for minimal left-right dark matter). The origin of neutrino mass and leptogenesis in these frameworks have been governed by a Dirac type Yukawa interaction term $y_\nu \overline{\ell_L} H N_R$. But the present $B-L$ extension of Standard Model with extra neutral fermions having exotic choice of $B-L$ charges can have potential stable cold dark matter candidates. The stability of dark matter is ensured by forbidding the generic interactions with SM leptons at renormalizable level and thereby, it can provide interesting dark matter phenomenology in both scalar and new gauge portal sector.

This manuscript is structured as: Sect. 2 follows the brief description of model and particle content along with the full Lagrangian and symmetry breaking. In Sect. 3, we discuss the neutrino masses and mixing with one sterile-like neutrino scenario and Sect. 4 includes the contribution of active-sterile mixing to the NDBD as per current experimental observation. In Sect. 5, we illustrate a detailed description of DM phenomenology and collider bounds on new gauge parameters within the model framework. In Sect. 6, we summarize and conclude the phenomenological consequences of the model.

Table 1 SM field content of lepton and Higgs sectors alongwith their corresponding charges

Field	L	e_R	μ_R	τ_R	H
$SU(2)_L$	2	1	1	1	2
A_4	3	1	$1''$	$1'$	1
$U(1)_{B-L}$	-1	-1	-1	-1	0
Z_3	1	ω^2	ω^2	ω^2	1

Table 2 Complete field content with their corresponding charges of the proposed model

Field	N_1	N_2	N_3	ϕ_2	ϕ_4	ϕ_8	ϕ_T	χ	ζ
$SU(2)_L$	1	1	1	1	1	1	1	1	1
A_4	1	1	1	1	1	1	3	3	$1'$
$U(1)_{B-L}$	5	-4	-4	2	4	8	0	0	0
Z_3	1	1	1	1	1	1	ω	1	1

2 Model description

We propose a new variant of $U(1)_{B-L}$ gauge extension of SM with additional A_4 flavor symmetry, which includes three new neutral fermions N_i's ($i = 1, 2, 3$) with exotic $B - L$ charges -4, -4 and $+5$ to nullify the triangle gauge anomalies [62]. This choice of adding three exotic fermions in the context of $B - L$ framework has been explored in several previous works [63–70]. The spontaneous symmetry breaking of $B - L$ gauge symmetry is realized by assigning non-zero vacuum expectation value (VEV) to three singlet scalars (ϕ_2, ϕ_4 and ϕ_8), which also generate mass terms to all exotic fermions and the new gauge boson. Additionally, A_4 flavor symmetry is used to study the neutrino phenomenology in this model. Apart from the usual SM Higgs doublet and the above mentioned three scalar singlets, which are responsible for electroweak and $U(1)_{B-L}$ gauge symmetry breaking respectively, there are three SM singlet flavon fields ϕ_T, χ, ζ to break the A_4 flavor symmetry at high scale. In the current framework, we chose the VEV of flavon fields to be much higher than the VEV of ϕ_2, ϕ_4 and ϕ_8 to explain the neutrino phenomenology. Finally we impose a Z_3 symmetry to forbid the unwanted terms in the interaction Lagrangian.

In this work, we intend to provide a detailed description of oscillation phenomenology with one sterile-like neutrino scenario. The complete field content with their corresponding charges are provided in Tables 1 and 2. The multiplication rules under A_4 symmetry group is outlined in Appendix.

2.1 Scalar potential and symmetry breaking pattern

Considering all the scalar content of the model, the potential can be written as

$$
\begin{aligned}
V =\ & \mu_H^2(H^\dagger H) + \lambda_H(H^\dagger H)^2 + \mu_2^2(\phi_2^\dagger \phi_2) \\
& + \lambda_{22}(\phi_2^\dagger \phi_2)^2 + \mu_4^2(\phi_4^\dagger \phi_4) + \lambda_4(\phi_4^\dagger \phi_4)^2 \\
& + \mu_8^2(\phi_8^\dagger \phi_8) + \lambda_8(\phi_8^\dagger \phi_8)^2 + \mu_T^2(\phi_T^\dagger \phi_T) \\
& + \lambda_T(\phi_T^\dagger \phi_T)^2 + \mu_\chi^2(\chi^\dagger \chi) + \lambda_\chi(\chi^\dagger \chi)^2 \\
& + \mu_\zeta^2(\zeta^\dagger \zeta) + \lambda_\zeta(\zeta^\dagger \zeta)^2 + \lambda_{H2}(H^\dagger H)(\phi_2^\dagger \phi_2) \\
& + \lambda_{H4}(H^\dagger H)(\phi_4^\dagger \phi_4) + \lambda_{H\chi}(H^\dagger H)(\chi^\dagger \chi) \\
& + \lambda_{H\zeta}(H^\dagger H)(\zeta^\dagger \zeta) + \lambda_{H8}(H^\dagger H)(\phi_8^\dagger \phi_8) \\
& + \lambda_{HT}(H^\dagger H)(\phi_T^\dagger \phi_T) + \lambda_{24}(\phi_2^\dagger \phi_2)(\phi_4^\dagger \phi_4) \\
& + \lambda_{28}(\phi_2^\dagger \phi_2)(\phi_8^\dagger \phi_8) + \lambda_{2T}(\phi_2^\dagger \phi_2)(\phi_T^\dagger \phi_T) \\
& + \lambda_{2\zeta}(\phi_2^\dagger \phi_2)(\zeta^\dagger \zeta) + \lambda_{2\chi}(\phi_2^\dagger \phi_2)(\chi^\dagger \chi) \\
& + \lambda_{48}(\phi_4^\dagger \phi_4)(\phi_8^\dagger \phi_8) + \lambda_{4T}(\phi_4^\dagger \phi_4)(\phi_T^\dagger \phi_T) \\
& + \lambda_{4\chi}(\phi_4^\dagger \phi_4)(\chi^\dagger \chi) + \lambda_{4\zeta}(\phi_4^\dagger \phi_4)(\zeta^\dagger \zeta) \\
& + \lambda_{8T}(\phi_8^\dagger \phi_8)(\phi_T^\dagger \phi_T) + \lambda_{8\chi}(\phi_8^\dagger \phi_8)(\chi^\dagger \chi) \\
& + \lambda_{8\zeta}(\phi_8^\dagger \phi_8)(\zeta^\dagger \zeta) + \lambda_{\chi T}(\chi^\dagger \chi)(\phi_T^\dagger \phi_T) \\
& + \lambda_{\chi\zeta}(\chi^\dagger \chi)(\zeta^\dagger \zeta) \\
& + \lambda_{\zeta T}(\zeta^\dagger \zeta)(\phi_T^\dagger \phi_T) + \mu_{24}\left((\phi_2)^2\phi_4^\dagger + (\phi_2^\dagger)^2\phi_4\right) \\
& + \lambda_{248}\left((\phi_2)^2\phi_4\phi_8^\dagger + (\phi_2^\dagger)^2\phi_4^\dagger\phi_8\right) \\
& + \mu_{48}\left((\phi_4)^2\phi_8^\dagger + (\phi_4^\dagger)^2\phi_8\right).
\end{aligned}
\tag{1}
$$

Moving towards symmetry breaking pattern, first the A_4 flavor symmetry is broken by the flavon fields. Then, the spontaneous breaking of $B - L$ gauge symmetry is implemented by assigning non-zero VEV to the scalar singlets ϕ_2, ϕ_4 and ϕ_8. Finally, the Higgs doublet breaks the SM gauge symmetry to a low energy theory. The VEV alignment of the flavons are chosen for a specific case, where the solution of such VEV structures are described in various literature [71–75] and are denoted as follows

$$
\begin{aligned}
& \langle H \rangle = \frac{v}{\sqrt{2}}\begin{pmatrix} 0 \\ 1 \end{pmatrix}, \quad \langle \phi_2 \rangle = \frac{v_2}{\sqrt{2}}, \\
& \langle \phi_4 \rangle = \frac{v_4}{\sqrt{2}}, \quad \langle \phi_8 \rangle = \frac{v_8}{\sqrt{2}}, \\
& \langle \phi_T \rangle = \frac{v_T}{\sqrt{2}}\begin{pmatrix} 1 \\ 0 \\ 0 \end{pmatrix}, \quad \langle \chi \rangle = \frac{v_\chi}{\sqrt{2}}\begin{pmatrix} 1 \\ 1 \\ 1 \end{pmatrix}.
\end{aligned}
\tag{2}
$$

2.2 CP-odd and CP-even scalar mass matrices

The scalar fields $H = (H^+, H^0)^T$ and ϕ_i, ($i = 2, 4, 8$) can be parametrized in terms of real scalars (h_i) and pseudo scalars (A_i) as

$$H^0 = \frac{1}{\sqrt{2}}(v + h) + \frac{i}{\sqrt{2}}A^0,$$

$$\phi_i^0 = \frac{1}{\sqrt{2}}(v_i + h_i) + \frac{i}{\sqrt{2}}A_i, \tag{3}$$

where v and v_i's are the corresponding vacuum expectation values. The CP-even component, h of the scalar doublet H, is considered to be the observed Higgs boson at LHC with mass $M_h = 125$ GeV. We neglect the mixing of Higgs with the new CP-even scalars, h_2, h_4 and h_8 (corresponding to ϕ_2, ϕ_4 and ϕ_8). The mass matrix in the basis (h_2, h_4, h_8) takes the form

$$M_E^2 = \begin{pmatrix} 2\lambda_{22}v_2^2 & v_2\left(\sqrt{2}\mu_{24} + \lambda_{24}v_4 + \lambda_{248}v_8\right) & v_2(\lambda_{248}v_4 + \lambda_{28}v_8) \\ v_2\left(\sqrt{2}\mu_{24} + \lambda_{24}v_4 + \lambda_{248}v_8\right) & 2\lambda_4 v_4{}^2 - \frac{v_2^2\left(\sqrt{2}\mu_{24} + \lambda_{248}v_8\right)}{2v_4} & \frac{\lambda_{248}v_2^2}{2} + v_4\left(\sqrt{2}\mu_{48} + \lambda_{48}v_8\right) \\ v_2\left(\lambda_{248}v_4 + \lambda_{28}v_8\right) & \frac{\lambda_{248}v_2^2}{2} + v_4\left(\sqrt{2}\mu_{48} + \lambda_{48}v_8\right) & 2\lambda_8 v_8{}^2 - \frac{\left(\sqrt{2}\mu_{48}v_4^2 + \lambda_{248}v_2^2 v_4\right)}{2v_8} \end{pmatrix}. \tag{4}$$

The diagonalization of the above mass matrix results the mass eigenstates, represented by H_1', H_2' and H_3' with masses $M_{H_1'}$, $M_{H_2'}$, $M_{H_3'}$ respectively. Moving to the CP-odd components, A_2, A_4 and A_8 (corresponding to ϕ_2, ϕ_4 and ϕ_8), the mass matrix in the basis (A_2, A_4, A_8) is given by

$$M_O^2 = \begin{pmatrix} -2v_4\left(\sqrt{2}\mu_{24} + \lambda_{248}v_8\right) & v_2\left(\sqrt{2}\mu_{24} - \lambda_{248}v_8\right) & \lambda_{248}v_2 v_4 \\ v_2\left(\sqrt{2}\mu_{24} - \lambda_{248}v_8\right) & -\frac{\left(\sqrt{2}\mu_{24} + \lambda_{248}v_8\right)v_2^2}{2v_4} - 2\sqrt{2}\mu_{48}v_8 & \frac{\lambda_{248}v_2^2}{2} + \sqrt{2}\mu_{48}v_4 \\ \lambda_{248}v_2 v_4 & \frac{\lambda_{248}v_2^2}{2} + \sqrt{2}\mu_{48}v_4 & -\frac{v_4\left(\lambda_{248}v_2^2 + \sqrt{2}\mu_{48}v_4\right)}{2v_8} \end{pmatrix}. \tag{5}$$

The above mass matrix upon diagonalization, gives one massless eigenstate, to be absorbed by $U(1)$ boson, Z' and two massive modes (represented by A_1' and A_2' with masses $M_{A_1'}$ and $M_{A_2'}$ respectively), which remain as massive physical CP-odd scalars in the present framework. The gauge boson Z' attains the mass $M_{Z'} = g_{BL}(4v_2^2 + 16v_4^2 + 64v_8^2)^{1/2}$.

2.3 Lagrangian and Leptonic Mass matrix

The Yukawa interaction Lagrangian for charged leptons, allowed by the symmetries of the model is as follows

$$\mathcal{L}_\ell = -H\left[\frac{y_e}{\Lambda}\left(\overline{L_L}\phi_T\right)_1 \otimes e_R \right.$$
$$\left. + \frac{y_\mu}{\Lambda}\left(\overline{L_L}\phi_T\right)_{1'} \otimes \mu_R + \frac{y_\tau}{\Lambda}\left(\overline{L_L}\phi_T\right)_{1''} \otimes \tau_R\right] + \text{H.c.} \tag{6}$$

The charged lepton mass matrix can be obtained from the above Lagrangian, which is written as follows,

$$\mathcal{M}_\ell = \begin{pmatrix} \frac{y_e v v_T}{2\Lambda} & 0 & 0 \\ 0 & \frac{y_\mu v v_T}{2\Lambda} & 0 \\ 0 & 0 & \frac{y_\tau v v_T}{2\Lambda} \end{pmatrix}. \tag{7}$$

Here, we use the VEV alignment of the flavon field ϕ_T as shown in Eq. (2). The ratio of expectation value of ϕ_T to the cut-off scale Λ (i.e., $\frac{v_T}{\Lambda}$) is considered to be $\sim \mathcal{O}(0.1)$ for the typical scale $\Lambda \sim \mathcal{O}(10^9)$ GeV. The Yukawa couplings y_e, y_μ and y_τ are assumed to be hierarchical to get the appropriate masses for the charged leptons.

With the absence of right-handed neutrinos (ν_R) with $B - L$ charge -1, there is no generic Dirac neutrino mass term i.e., $\bar{L}\tilde{H}\nu_R$ in the present framework. In addition, we cannot write the Dirac and Majorana mass terms for light active neutrinos with the exotic fermions at tree level. Also the well known dimension-5 Weinberg operators ($\frac{LLHH}{\Lambda}$) are not allowed, as these terms are not invariant under $\hat{U}(1)_{B-L}$ gauge symmetry. Therefore, the neutral lepton masses are generated by the dimension six and seven operators. We thus obtain the Majorana mass terms for the neutrinos as

$$\mathcal{L}_\nu = -\frac{y_1}{\Lambda^2}[LLHH]_1 \otimes \phi_2 - \frac{y_\chi}{\Lambda^3}[LLHH]_3 \otimes \chi \otimes \phi_2. \tag{8}$$

After the spontaneous symmetry breaking, the 3×3 mass matrix for active neutrinos takes the form

$$\mathcal{M}_\nu = \begin{pmatrix} a + \frac{2d}{3} & -\frac{d}{3} & -\frac{d}{3} \\ -\frac{d}{3} & \frac{2d}{3} & a - \frac{d}{3} \\ -\frac{d}{3} & a - \frac{d}{3} & \frac{2d}{3} \end{pmatrix}, \tag{9}$$

where, $a = \frac{y_1 v_2 v^2}{2\sqrt{2}\Lambda^2}$ and $d = \frac{y_\chi v_\chi v^2 v_2}{4\Lambda^3}$. The sub-eV scale light neutrinos can be obtained from the representative set of input model parameters as follows: $v = 246$ GeV, $\frac{v_\chi}{\Lambda} \approx 0.2$, $v_2 \approx \mathcal{O}(10^3)$ GeV and $y_1 \approx y_\chi \approx \mathcal{O}(1)$. The flavor structure of the matrix $\mathcal{M}_\nu$ obtained from A_4 symmetry is known to

be diagonalized by the TBM mixing matrix [76], which is given by

$$
U_{\text{TBM}} = \begin{pmatrix} -\sqrt{\frac{2}{3}} & \sqrt{\frac{1}{3}} & 0 \\ \sqrt{\frac{1}{6}} & \sqrt{\frac{1}{3}} & -\sqrt{\frac{1}{2}} \\ \sqrt{\frac{1}{6}} & \sqrt{\frac{1}{3}} & \sqrt{\frac{1}{2}} \end{pmatrix}.
\tag{10}
$$

The standard scenario of three neutrinos gives a TBM mixing pattern with vanishing reactor mixing angle in the framework of A_4 flavor symmetry, which has been studied in various works in the literature [77–82]. In the next section we consider the active-sterile neutrino mixing by introducing an eV scale sterile-like neutrino and discuss the diagonalization of 4×4 mass matrix to account for nonzero reactor mixing angle, consistent with current neutrino oscillation data.

3 Neutrino masses and mixing with one eV scale sterile-like neutrino

The standard scenario of three neutrino species has already been widely discussed in the literature, but the current experimental discrepancies from MiniBooNE and LSND data hint towards the possible existence of the fourth neutrino. From the nomenclature of the sterile neutrinos, one can infer that it doesn't interact with the SM particles directly as it does not have gauge interaction, instead mixes with the active neutrinos during oscillation. The mixing between the flavor (ν_f) and mass eigenstates (ν_i) are related by

$$
\nu_f = \sum_{i=1}^{n} U_i \nu_i.
\tag{11}
$$

where n denotes the number of neutrino species. By considering three generations of active neutrinos, along with n_s number of massive sterile species, one can have $n = 3 + n_s$ dimensional neutrino mixing matrix. In general, the mixing matrix will have $n - 1 = n_s + 2$ Majorana phases, $3 \times (n-2) = 3 \times (n_s+1)$ mixing angles and $2n-5 = 2n_s+1$ Dirac phases. Hence, in one sterile neutrino scenario, we will have 6 mixing angles, 3 Dirac phases and 3 Majorana phases. The standard parameterization for 4×4 neutrino mixing is given by

$$
U = R_{34}\tilde{R}_{24}\tilde{R}_{14}R_{23}\tilde{R}_{13}R_{12}P,
\tag{12}
$$

where the matrices R_{ij} are rotations in ij space and have the form

Table 3 2σ estimated values of the mixing parameters in one sterile neutrino scenario [10]

	Parameter	Δm_{41}^2 [eV]	$|U_{e4}|^2$
3+1/1+3	best-fit	1.78	0.023
	2σ	1.61–2.01	0.006–0.040

$$
R_{34} = \begin{pmatrix} 1 & 0 & 0 & 0 \\ 0 & 1 & 0 & 0 \\ 0 & 0 & c_{34} & s_{34} \\ 0 & 0 & -s_{34} & c_{34} \end{pmatrix}, \ \tilde{R}_{14}
$$

$$
= \begin{pmatrix} c_{14} & 0 & 0 & s_{14}e^{-i\delta_{14}} \\ 0 & 1 & 0 & 0 \\ 0 & 0 & 1 & 0 \\ -s_{14}e^{i\delta_{14}} & 0 & 0 & c_{14} \end{pmatrix}, \ \tilde{R}_{24}
$$

$$
= \begin{pmatrix} 1 & 0 & 0 & 0 \\ c_{24} & 0 & 0 & s_{24}e^{-i\delta_{24}} \\ 0 & 0 & 1 & 0 \\ -s_{24}e^{i\delta_{24}} & 0 & 0 & c_{24} \end{pmatrix}.
\tag{13}
$$

Here, $s_{ij} = \sin\theta_{ij}$, $c_{ij} = \cos\theta_{ij}$ and P denotes the diagonal matrix with three Majorana phases α, β and γ,

$$
P = \text{diag}\left(1, e^{i\alpha/2}, e^{i(\beta/2+\delta_{13})}, e^{i(\gamma/2+\delta_{14})}\right).
\tag{14}
$$

The current experimental searches of light sterile neutrino prefer a larger value of active-sterile mass squared differences than the observed solar and atmospheric mass squared differences of active neutrino oscillation. This implies that the mass for sterile neutrino can be either heavier or lighter than the active ones. We know that in normal ordering the active neutrinos have the form $m_3 \gg m_2 > m_1$ whereas, the inverse ordering is given by $m_2 > m_1 \gg m_3$). So accordingly, there will be four possibilities in mass orderings if a sterile neutrino is added to the framework. Following the top to bottom nomenclature, i.e. if $m_s \gg m_{1,2,3}$, can be denoted as 1+3 scenario for normal or inverted ordering of the active neutrinos. Whereas, if the case is reversed, i.e. if sterile state is lighter than the active ones ($m_{1,2,3} \gg m_s$), this configuration is named as 3+1 model in literature. Moreover, less attention is given to 3+1 scenario as they are prone to conflict with several experimental observations. In this model, we consider 1+3 like scenarios, to explain the neutrino phenomenology with eV scale exotic fermion.

Table 3 shows the best-fit and 2σ ranges of the relevant oscillation parameters, we used for this work.

3.1 Diagonalization of Neutrino mass matrix in $3 + 1$ like scenario

Out of the three exotic fermions, we consider the fermion with $B - L$ charge 5 to mix with the SM neutrinos, to

study the neutrino phenomenology analogous to the mixing between the standard and sterile neutrinos $3 + 1$ mixing scenario. The Majorana mass terms for fermions and their interaction with SM leptons are given by

$$L_N = -\left[\frac{y_{11}}{\Lambda}\left(N_1 N_1 \phi_8^\dagger \phi_2^\dagger\right)\right.$$
$$\left. + \frac{y_s}{\Lambda^3}\left(\bar{L}\tilde{H}N_1(\phi_4^\dagger \phi_2^\dagger + \phi_8^\dagger \phi_2)\chi\right) + \text{H.c.}\right]. \quad (15)$$

Here, the first and second terms are for eV scale Majorana mass for sterile-like neutrino, generated from dimension 5 and 7 operators respectively. The dimension 7 operator in the third term induces active-sterile neutrino mixing. Thus the resulting 4×4 neutrino mass matrix is given as follows

$$\mathcal{M}_\nu = \begin{pmatrix} a + \frac{2d}{3} & -\frac{d}{3} & -\frac{d}{3} & e \\ -\frac{d}{3} & \frac{2d}{3} & a - \frac{d}{3} & e \\ -\frac{d}{3} & a - \frac{d}{3} & \frac{2d}{3} & e \\ e & e & e & m_s \end{pmatrix}. \quad (16)$$

Here, $e = \frac{y_s v(v_4+v_8)v_2 v_\chi}{4\Lambda^3}$ and $m_s \approx \frac{y_{11}v_2 v_8}{2\Lambda}$ (neglecting the contributions from dim-6 operators), are related to the active-sterile mixing parameter (e/m_s) and Majorana mass of the sterile-like fermion respectively. The eV scale mass of the sterile neutrino (m_s) and sub-eV scale parameter, responsible for the active-sterile neutrino mixing (e) can be generated with the following representative set of input model parameters: $y_{11} \approx \mathcal{O}(10^{-6})$, $y_s \approx \mathcal{O}(1)$, $v_2 = v_4 = v_8 \simeq \mathcal{O}(10^3)$ GeV and $\frac{v_\chi}{\Lambda} \approx 0.2$. The above mass matrix is analytically diagonalized to get the physical masses of $3 + 1$ neutrinos and the eigenvector matrix is given as

$$U = \begin{pmatrix} \frac{2}{\sqrt{6}} & \frac{1}{6e}\frac{K_-}{N_-} & 0 & \frac{1}{6e}\frac{K_+}{N_+} \\ -\frac{1}{\sqrt{6}} & \frac{1}{6e}\frac{K_-}{N_-} & -\frac{1}{\sqrt{2}} & \frac{1}{6e}\frac{K_+}{N_+} \\ -\frac{1}{\sqrt{6}} & \frac{1}{6e}\frac{K_-}{N_-} & \frac{1}{\sqrt{2}} & \frac{1}{6e}\frac{K_+}{N_+} \\ 0 & \frac{1}{N_-} & 0 & \frac{1}{N_+} \end{pmatrix}, \quad (17)$$

where, $K_\pm = a - m_s \pm \sqrt{12e^2 + (a - m_s)^2}$ and $N_\pm^2 = 1 + \frac{\left(a - m_s \pm \sqrt{12e^2 + (a-m_s)^2}\right)^2}{12e^2}$. If one assumes that $a < m_s$ and expands to second order in the small ratio e/m_s, the resulting mixing matrix is given by [20]

$$U \simeq \begin{pmatrix} \frac{2}{\sqrt{6}} & \frac{1}{\sqrt{3}} & 0 & 0 \\ -\frac{1}{\sqrt{6}} & \frac{1}{\sqrt{3}} & -\frac{1}{\sqrt{2}} & 0 \\ -\frac{1}{\sqrt{6}} & \frac{1}{\sqrt{3}} & \frac{1}{\sqrt{2}} & 0 \\ 0 & 0 & 0 & 1 \end{pmatrix} + \begin{pmatrix} 0 & 0 & 0 & \frac{e}{m_s} \\ 0 & 0 & 0 & \frac{e}{m_s} \\ 0 & 0 & 0 & \frac{e}{m_s} \\ 0 & -\frac{\sqrt{3}e}{m_s} & 0 & 0 \end{pmatrix}$$
$$+ \begin{pmatrix} 0 & -\frac{\sqrt{3}e^2}{2m_s^2} & 0 & 0 \\ 0 & -\frac{\sqrt{3}e^2}{2m_s^2} & 0 & 0 \\ 0 & -\frac{\sqrt{3}e^2}{2m_s^2} & 0 & 0 \\ 0 & 0 & 0 & -\frac{3e^2}{2m_s^2} \end{pmatrix}. \quad (18)$$

But this mixing pattern predicts $\theta_{13} = 0$, which has already been experimentally ruled out. Hence, to explain the non-zero θ_{13}, we introduce one extra flavon field ζ, which is charged as $1'$ under A_4 symmetry, in order to perturb the neutrino mass matrix from the TBM mixing pattern. Including this new flavon field, the perturbed Lagrangian is given by

$$\mathcal{L}_p = -\frac{y_p}{\Lambda^3}\left([LLHH]_{1''} \otimes (\zeta)_{1'} \otimes \phi_2 + \text{H.c.}\right). \quad (19)$$

When the flavon field acquires VEV, $\langle\zeta\rangle = \frac{v_\zeta}{\sqrt{2}}$, the above term contributes to the mass matrix in (16). Hence, the modified neutrino mass matrix can be written as

$$\mathcal{M}_\nu = \begin{pmatrix} a + \frac{2d}{3} & -\frac{d}{3} & -\frac{d}{3} & e \\ -\frac{d}{3} & \frac{2d}{3} & a - \frac{d}{3} & e \\ -\frac{d}{3} & a - \frac{d}{3} & \frac{2d}{3} & e \\ e & e & e & m_s \end{pmatrix} + \begin{pmatrix} 0 & 0 & b & 0 \\ 0 & b & 0 & 0 \\ b & 0 & 0 & 0 \\ 0 & 0 & 0 & 0 \end{pmatrix}, \quad (20)$$

where, $b = \frac{y_p v^2 v_\zeta v_2}{4\Lambda^3}$. We choose $\frac{v_\zeta}{\Lambda} \approx \mathcal{O}(0.1)$ and $y_p \approx \mathcal{O}(1)$ in order to achieve a sub-eV scale for the parameter b. We analytically diagonalize the above mass matrix and the mixing matrix is constructed from the normalized eigenvectors, which takes the form

$$U = \begin{pmatrix} \frac{-p_+}{l_{p+}} & \frac{1}{6e}\frac{K_{p-}}{N_{p-}} & \frac{-p_-}{l_{p-}} & \frac{1}{6e}\frac{K_{p+}}{N_{p+}} \\ \frac{q_+}{l_{p+}} & \frac{1}{6e}\frac{K_{p-}}{N_{p-}} & \frac{q_-}{l_{p-}} & \frac{1}{6e}\frac{K_{p+}}{N_{p+}} \\ \frac{1}{l_{p+}} & \frac{1}{6e}\frac{K_{p-}}{N_{p-}} & \frac{1}{l_{p-}} & \frac{1}{6e}\frac{K_{p+}}{N_{p+}} \\ 0 & \frac{1}{N_{p-}} & 0 & \frac{1}{N_{p+}} \end{pmatrix}, \quad (21)$$

here,

$$K_{p\pm} = a + b - m_s \pm \sqrt{12e^2 + (a + b - m_s)^2},$$

$$N_{p\pm}^2 = 1 + \frac{\left(a + b - m_s \pm \sqrt{12e^2 + (a + b - m_s)^2}\right)^2}{12e^2},$$

$$p_\pm = \frac{a \pm \sqrt{a^2 - ab + b^2}}{a - b}, \qquad q_\pm = \frac{b \pm \sqrt{a^2 - ab + b^2}}{a - b},$$

$$l_{p\pm}^2 = 1 + (p_\pm)^2 + (q_\pm)^2. \tag{22}$$

And the mass eigenvalues of the 4×4 neutrino mixing matrix are stated as following

$$m_{\nu_1} = d + \sqrt{a^2 - ab + b^2},$$

$$m_{\nu_2} = \frac{1}{2}[a + b + m_s - \sqrt{12e^2 + (a + b - m_s)^2}],$$

$$m_{\nu_3} = d - \sqrt{a^2 - ab + b^2},$$

$$m_{\nu_4} = \frac{1}{2}[a + b + m_s + \sqrt{12e^2 + (a + b - m_s)^2}]. \tag{23}$$

Comparing with the standard 4×4 mixing matrix, we can have the mixing angles as follows

$$\sin^2 \theta_{12} = \frac{|U_{e2}|^2}{1 - |U_{e4}|^2} \simeq \frac{1}{3}\left[1 - 2\left(\frac{e}{m_s}\right)^2\right], \tag{24}$$

$$\sin^2 \theta_{23} = \frac{|U_{\mu3}|^2(1 - |U_{e4}|^2)}{1 - |U_{e4}|^2 - |U_{\mu4}|^2} \simeq \frac{1}{2}\left[1 + \left(\frac{e}{m_s}\right)^2\right], \tag{25}$$

$$\sin^2 \theta_{14} = |U_{e4}|^2 \approx \left(\frac{e}{m_s}\right)^2, \tag{26}$$

$$\sin \theta_{34} = \frac{|U_{\tau4}|^2}{1 - |U_{e4}|^2 - |U_{\mu4}|^2} \approx \left(\frac{e}{m_s}\right)^2, \tag{27}$$

$$\sin^2 \theta_{24} = \frac{|U_{\mu4}|^2}{1 - |U_{e4}|^2} \approx \left(\frac{e}{m_s}\right)^2, \tag{28}$$

$$\sin^2 \theta_{13} = \frac{|U_{e3}|^2}{(1 - \sin^2 \theta_{23})(1 - \sin^2 \theta_{14})}$$

$$= \frac{b^2}{4a^2}\left(1 + 2\frac{e^2}{m_s^2}\right). \tag{29}$$

From the above equations, we can infer that adding the perturbation term in the interaction Lagrangian gives non-zero θ_{13}, which is compatible with the current oscillation data.

3.2 Numerical analysis

To perform numerical analysis in a systematic way, we define $\lambda_1 = \frac{b}{a}$, $\lambda_2 = \frac{d}{a}$ and $\lambda_3 = \frac{e^2}{m_s a}$ with ϕ_{ba}, ϕ_{da}, ϕ_{ea} as the phases of λ_1, λ_2 and λ_3 respectively. The expressions of mass eigenvalues in (30) can thus be written as

$$m_{\nu_1} = |m_{\nu_1}|e^{i\phi_1} = |a|\left|\lambda_2 e^{i\phi_{da}} + \sqrt{1 - \lambda_1 e^{i\phi_{ba}} + \lambda_1^2 e^{2i\phi_{ba}}}\right|e^{i\phi_1},$$

$$m_{\nu_2} = |m_{\nu_2}|e^{i\phi_2} = |a|\left|1 + \lambda_1 e^{i\phi_{ba}} - 3\lambda_3 e^{i\phi_{ea}}\right|e^{i\phi_2},$$

$$m_{\nu_3} = |m_{\nu_3}|e^{i\phi_3} = |a|\left|\lambda_2 e^{i\phi_{da}} - \sqrt{1 - \lambda_1 e^{i\phi_{ba}} + \lambda_1^2 e^{2i\phi_{ba}}}\right|e^{i\phi_3},$$

$$m_{\nu_4} = |m_{\nu_4}|e^{i\phi_4} = |a|\left|\frac{m_s}{a} + 3\lambda_3 e^{i\phi_{ea}}\right|e^{i\phi_4}. \tag{30}$$

Thus, one obtains the physical masses as

$$|m_{\nu_1}| = |a|\left[(\lambda_2 \cos \phi_{da} + C)^2 + (\lambda_2 \sin \phi_{da} + D)^2\right]^{\frac{1}{2}},$$

$$|m_{\nu_2}| = |a|\left[(1 + \lambda_1 \cos \phi_{ba} - 3\lambda_3 \cos \phi_{ea})^2\right.$$

$$\left. + (\lambda_1 \sin \phi_{ba} - 3\lambda_3 \sin \phi_{ea})^2\right]^{\frac{1}{2}},$$

$$|m_{\nu_3}| = |a|\left[(\lambda_2 \cos \phi_{da} - C)^2 + (\lambda_2 \sin \phi_{da} - D)^2\right]^{\frac{1}{2}},$$

$$|m_{\nu_4}| = |a|\left[(\frac{m_s}{a} + 3\lambda_3 \cos \phi_{ea})^2 + (3\lambda_3 \sin \phi_{ea})^2\right]^{\frac{1}{2}}, \tag{31}$$

where,

$$C = \left(\frac{A + \sqrt{A^2 + B^2}}{2}\right)^{\frac{1}{2}}, \quad D = \left(\frac{-A + \sqrt{A^2 + B^2}}{2}\right)^{\frac{1}{2}},$$

$$A = 1 - \lambda_1 \cos \phi_{ba} + \lambda_1^2 \cos 2\phi_{ba},$$

$$B = -\lambda_1 \sin \phi_{ba} + \lambda_1^2 \sin 2\phi_{ba}. \tag{32}$$

The corresponding phases in the mass eigenvalues values are given by

$$\phi_1 = \tan^{-1}\left[\frac{\lambda_2 \sin \phi_{da} + D}{\lambda_2 \cos \phi_{da} + C}\right],$$

$$\phi_3 = \tan^{-1}\left[\frac{\lambda_2 \sin \phi_{da} - D}{\lambda_2 \cos \phi_{da} - C}\right],$$

$$\phi_2 = \tan^{-1}\left[\frac{\lambda_1 \sin \phi_{ba} - 3\lambda_3 \sin \phi_{ea}}{1 + \lambda_1 \cos \phi_{ba} - 3\lambda_3 \cos \phi_{ea}}\right],$$

$$\phi_4 = \tan^{-1}\left[\frac{3\lambda_3 \sin \phi_{ea}}{\frac{m_s}{a} + 3\lambda_3 \cos \phi_{ea}}\right]. \tag{33}$$

The model also predicts a large CP violating Dirac phase, associated with the non-zero reactor mixing angle, which can be obtained from (12)

$$\text{Exp}(-i\delta_{13}) = \frac{U_{13}}{\sin \theta_{13} \cos \theta_{14} \cos \theta_{23}} \approx \text{Exp}(i\phi_{ba}). \tag{34}$$

The above equation gives $\sin \delta_{13} \approx -\sin \phi_{ba}$. To constrain the model parameters, compatible with the 3σ limits of the current oscillation data, we perform a random scan of these parameters over the following ranges:

$$a \in [-0.06, 0.06] \text{ eV}, \quad e \in [-0.1, 0.1] \text{ eV},$$

$$m_s \in [-1.5, 1.5] \text{ eV}, \quad \lambda_1 \in [0.01, 0.3],$$

$$\lambda_2 \in [0.01, 0.5], \quad \phi_{ba,da,ea} \in [-\pi, \pi], \tag{35}$$

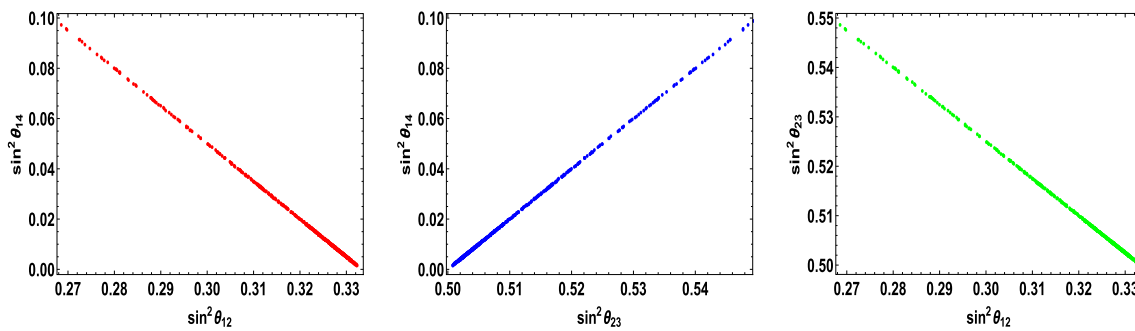**Fig. 1** Correlation of the active-sterile mixing angle θ_{14} with solar mixing angle θ_{12} (left panel), with atmospheric mixing angle θ_{23} (middle panel) and between the atmospheric and solar mixing angles (right panel)

and show the correlation plots between different mixing angles in Fig. 1. We now proceed to discuss explicitly the constraints on different parameters from the availed neutrino oscillation data for vanishing and non-vanishing Dirac CP phase, by fixing various model parameters. Firstly we filter the parameters from the constraints of observed solar and atmospheric mass squared differences in 3σ range and then the obtained parameter space is further constrained from the cosmological observation of total neutrino mass.

3.2.1 Variation of model parameters by fixing $\lambda_2 = 0.5$ and $\phi_{ba} = 0$

We discuss the dependence of various model parameters, which are consistent with the 3σ allowed ranges of neutrino oscillation observables. The correlation and constraints on these parameters are presented in Figs. 2, 3, 4, 5. Here, we fix $\lambda_2 = 0.5$ and the phase associated with λ_1, $\phi_{ba} = 0$. We vary λ_1 from 0.01 to 0.3, which in turn gives a favorable parameter space for λ_1 to lie within 0.25 to 0.3, allowed by the 3σ observation of θ_{13}, which is more stringent than the constraint from total active neutrino mass as shown in the left panel of Fig. 2. From the right panel, the allowed region for $|\lambda_3|$ turns out to be in the range 0.1 to 0.6. We found Majorana like phases ϕ_1, ϕ_2 and ϕ_3 to have the allowed values of $[-0.18, 0.18]\pi$ (top-left panel), $[-0.5, 0.5]\pi$ (top-right panel) and $[-0.09, 0.09]\pi$ (bottom panel) of Fig. 3. Similarly, the left panel of Fig. 4 represents a strong constraint on the parameter **a** from cosmological observation of total active neutrino mass, which would lie within a range of ± 0.035 to ± 0.05 eV and the correlation of $|U_{e4}|^2$ with Δm_{41}^2 (eV^2) is shown in the right panel. The phases of λ_2 and λ_3, i.e., ϕ_{da} and ϕ_{ea} are strongly constrained from neutrino mass bound. These phases are found to lie in the range, ± 2.4 to ± 3.14 and $(-1$ to $+1$ and ± 2.5 to $\pm 3.14)$ radians respectively, as shown in the left and right panels of Fig. 5. In the present case, by fixing $\phi_{ba} = 0$, one can have a vanishing δ_{13}, even though θ_{13} remains non-zero as seen from Eq. (34).

3.2.2 Variation of model parameters by fixing $\lambda_2 = 0.5$ and $\phi_{ba} \neq 0$

In the previous case, we have a vanishing CP phase ($\delta_{13} = -\phi_{ba}$), here, we try to show the impact of non-zero δ_{13} on the model parameters. We consider the phase of λ_1, ϕ_{ba} to vary from $-\pi$ to π, which changes the allowed region of model parameters, described in the previous case. From the left panel of Fig. 6, we found that the region $-0.6 < \lambda_3 < 0.6$ is allowed by the cosmological bound on sum of active neutrino masses and the right panel shows the constraint on **a** which is $\pm[0.03, 0.045]$, slightly more stringent than the previous case. The parameter scan for ϕ_{da} (in radian) to lie within the domain ± 2.4 to ± 3.14 as shown in the left panel of Fig. 7. The favored parameter space for ϕ_{ea} is represented in the right panel, which allows the values of -3.14 to 3.14 (in radians). The correlation of CP phase δ_{13} and ϕ_1 with parameter **a** are shown in the left and right panels of Fig. 8. In this case, we found that the other parameters do not change appreciably in comparison with the previous case.

4 Discussion on neutrinoless double beta decay with eV-scale neutrinos.

To accommodate an eV scale sterile-like neutrino N_1, with lepton number violating (LNV) Majorana mass manifest the new physics contribution beyond SM [85–88]. The well known process of NDBD includes the simultaneous decay of two neutrons from the nucleus of an isotope (A, Z) into two protons and two electrons without the emission of any neutrinos in the final state [89–93],

$$(A, Z) \rightarrow (A, Z+2)^{++} + 2e^-.$$

The half-life for a given isotope can be expressed in terms of phase-space factor $\mathcal{G}_{(A, Z)}^{0\nu}$, nuclear matrix element $\mathcal{M}_{(A, Z)}^{0\nu}$ (presented in Table.5) and dimensionless effective parameter $\eta_{\text{eff}}^{0\nu}$, which can be inferred from the following expression,

Table 4 The experimental values of Neutrino oscillation parameters for 1σ, 2σ and 3σ range [83,84]

Parameter	Best fit $\pm 1\sigma$	2σ range	3σ range
Δm_{21}^2 $[10^{-5}\text{eV}^2]$	7.56 ± 0.19	7.20–7.95	7.05–8.14
$|\Delta m_{31}^2|$ $[10^{-3}\text{eV}^2]$ (NO)	2.55 ± 0.04	2.47–2.63	2.43–2.67
$|\Delta m_{31}^2|$ $[10^{-3}\text{eV}^2]$ (IO)	$2.47^{+0.04}_{-0.05}$	2.39–2.55	2.34–2.59
$\sin^2\theta_{12}/10^{-1}$	$3.21^{+0.18}_{-0.16}$	2.89–3.59	2.73–3.79
$\sin^2\theta_{23}/10^{-1}$ (NO)	$4.30^{+0.20}_{-0.18}$	3.98–4.78 & 5.60–6.17	3.84–6.35
$\sin^2\theta_{23}/10^{-1}$ (IO)	$5.98^{+0.17}_{-0.15}$	4.09–4.42 & 5.61–6.27	3.89–4.88 & 5.22–6.41
$\sin^2\theta_{13}/10^{-2}$ (NO)	$2.155^{+0.090}_{-0.075}$	1.98–2.31	1.89–2.39
$\sin^2\theta_{13}/10^{-2}$ (IO)	$2.155^{+0.076}_{-0.092}$	1.98–2.31	1.90–2.39

Fig. 2 The left panel shows the dependence of the reactor mixing angle θ_{13} on λ_1 and right panel represents the correlation between the sum of total active neutrino masses and λ_3
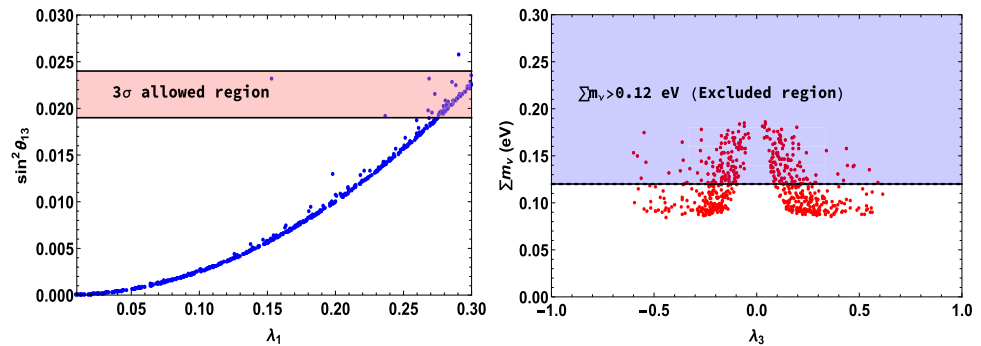
Fig. 3 Correlation between ϕ_1 (top-left panel), ϕ_2 (top-right panel) and ϕ_3 (bottom) with the total active neutrino mass
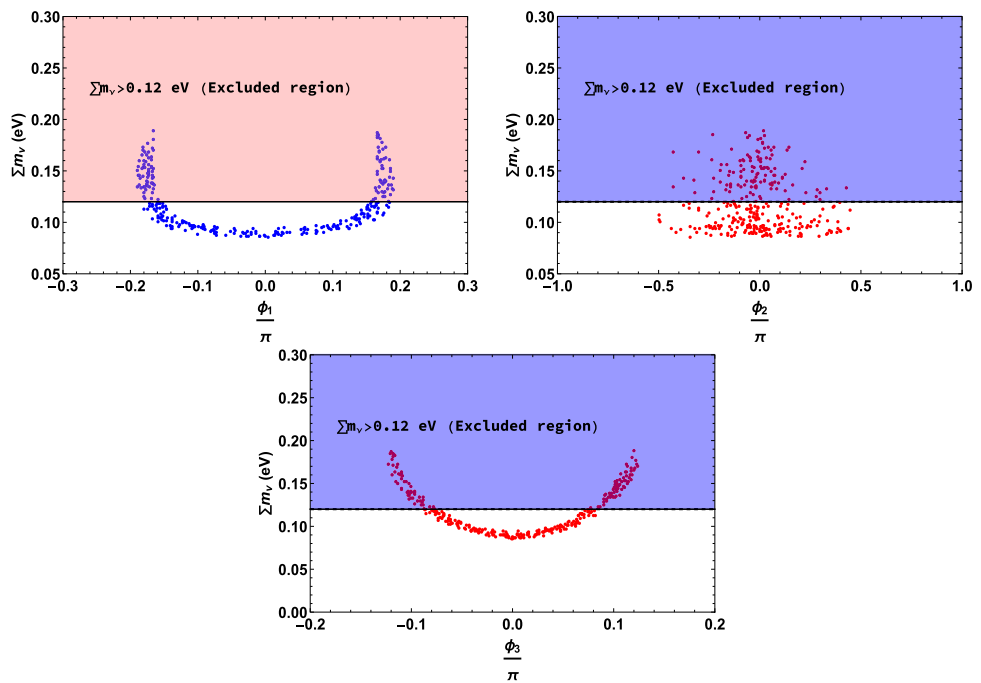
$$(T_{1/2}^{0\nu})_{(A,Z)}^{-1} = \mathcal{G}_{(A,Z)}^{0\nu}|\mathcal{M}_{(A,Z)}^{0\nu}\eta_{\text{eff}}^{0\nu}|^2. \tag{36}$$

The experimental observation of $0\nu\beta\beta$ process will indicate the existence of an (effective) LNV operator. We discuss here the standard mechanism and new physics contribution to this rare process in the present framework with eV scale sterile-like neutrino.

The process mediated by SM light neutrinos, which are Majorana in nature, is shown in Fig. 9 (left panel). The dimensionless parameter, responsible for LNV is given by the *ee* element of the Majorana mass matrix, normalized by the

Fig. 4 Left panel projects the variation of model parameter **a** with total active neutrino mass and right panel represents the variation of ϕ_2 with total active neutrino mass
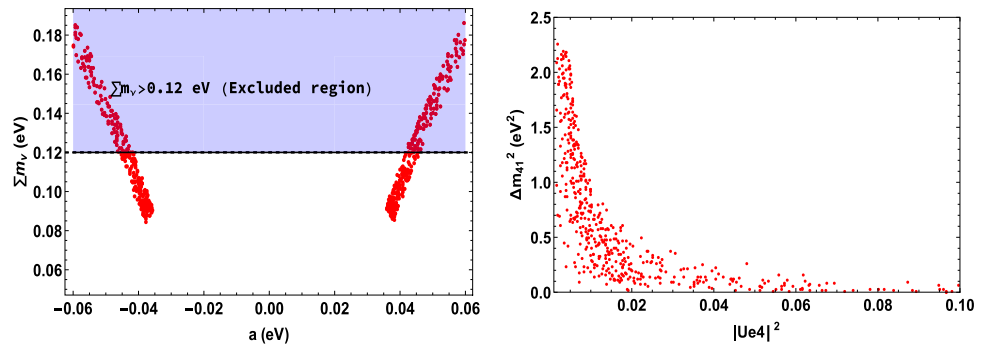
Fig. 5 Left (Right) panel represents the variation of ϕ_{da} (ϕ_{ea}) with total active neutrino mass
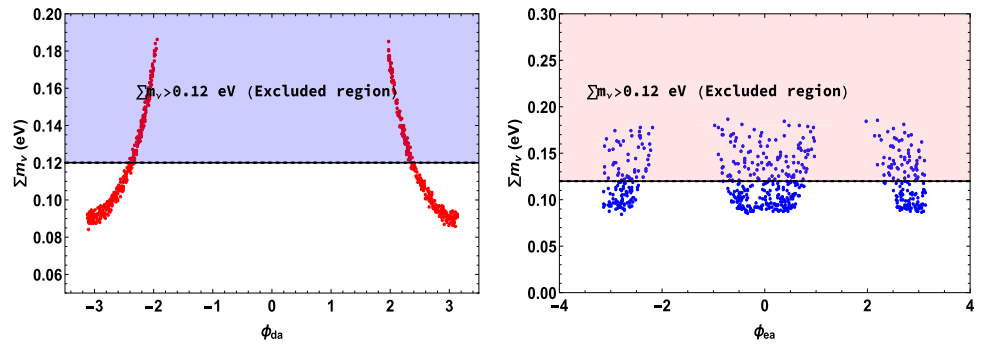
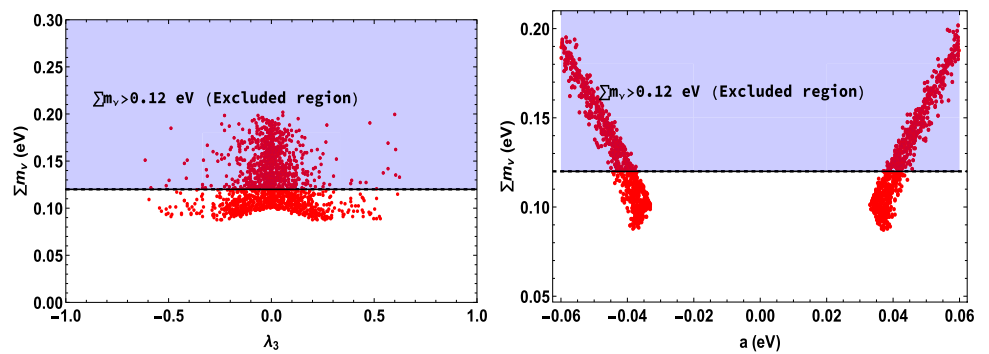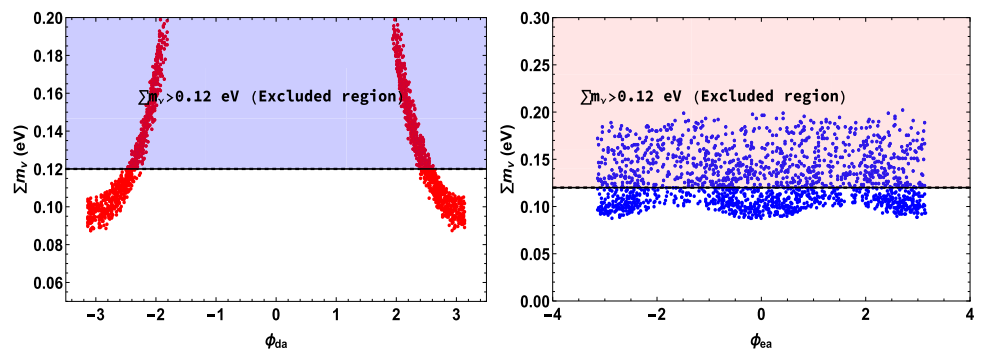**Fig. 6** Left (Right) panel shows the variation of λ_3 (**a**) with total active neutrino masses

Fig. 7 Left (Right) panel shows the variation of ϕ_{da} (ϕ_{ea}) with total active neutrino masses

electron mass as,

$$\eta_{\text{eff}}^{0\nu} \equiv \frac{m_{ee}^{\nu}}{m_e} = \frac{1}{m_e}\left(\sum_{i=1}^{3}(U_{\text{PMNS}})_{ei}^2\, m_i\right). \tag{37}$$

where U_{PMNS} is the unitary PMNS mixing matrix and m_i is the mass eigenvalues of the light active neutrinos.

The parametrisation of the PMNS mixing matrix U_{PMNS} is given by

$$U_{\text{PMNS}} = \begin{pmatrix} 1 & 0 & 0 \\ 0 & c_{23} & s_{23} \\ 0 & -s_{23} & c_{23} \end{pmatrix} \begin{pmatrix} c_{13} & 0 & s_{13}e^{-i\delta} \\ 0 & 1 & 0 \\ -s_{13}e^{i\delta} & 0 & c_{13} \end{pmatrix}$$

$$\times \begin{pmatrix} c_{12} & s_{12} & 0 \\ -s_{12} & c_{12} & 0 \\ 0 & 0 & 1 \end{pmatrix} \begin{pmatrix} 1 & 0 & 0 \\ 0 & e^{\frac{i\alpha}{2}} & 0 \\ 0 & 0 & e^{\frac{i\beta}{2}} \end{pmatrix} \tag{38}$$

Fig. 8 Left panel shows the variation of **a** with the Dirac like CP phase and the right panel depicts the correlation between **a** and ϕ_1
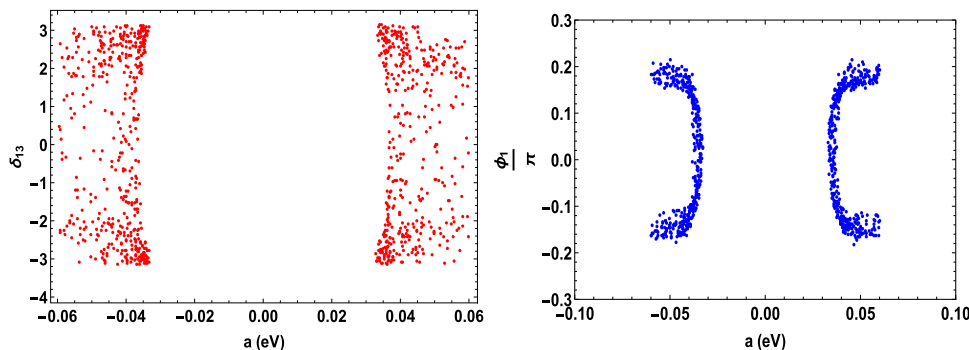
Table 5 The numerical values of the phase-space factor and nuclear matrix elements

Isotope	$G_{0\nu}[10^{-15}\text{ yrs}^{-1}]$	$\mathcal{M}_\nu$
^{76}Ge	7.98	3.85–5.82
^{136}Xe	59.2	2.19–3.36

where $c_{ij} = \cos\theta_{ij}$, $s_{ij} = \sin\theta_{ij}$ are sine and cosine of the mixing angles, δ is the Dirac CP-phase and α, β are Majorana phases. Using the above mixing matrix U_{PMNS} in eq.(37), the modified effective Majorana mass can be read as,

$$m^\nu_{ee} = \left| m_1 c^2_{12} c^2_{13} + m_2 s^2_{12} c^2_{13} e^{i\alpha} + m_3 s^2_{13} e^{i\beta} \right| \qquad (39)$$

The effective Majorana mass depends upon the neutrino oscillation parameter θ_{12}, θ_{13} and the neutrino mass eigenvalues m_1, m_2 and m_3 and phases. However, we do not know the absolute value of these light neutrino masses but neutrino oscillation experiments gives mass squared difference between them. Also we have no information about these phases. In our analysis, we randomly vary these phases and took 3σ range of neutrino oscillation parameters to see whether we can get any crucial information about absolute scale of neutrino masses and mass ordering using experimental limit from neutrinoless double beta decay experiments.

We definitely know sign of $\Delta m^2_{sol}(\equiv \Delta m^2_{21}) = m^2_2 - m^2_1$ is positive which implies $m_2 > m_1$. But neutrino oscillation experiments can not provide unambiguous sign of

$m^2_{atm}(\Delta m^2_{31})$ which allows two possible ordering of neutrino mass as,

$$\Delta m^2_{atm}(\Delta m^2_{31}) = m^2_3 - m^2_1, \text{ for Normal Hierarchy(NH)}$$
$$= m^2_1 - m^2_3, \text{ for Inverted Hierarchy (IH)}$$

Normal Hierarchy (NH) : $m_1 < m_2 \ll m_3$

Here, $m_1 = m_{\text{lightest}}$; $m_2 = \sqrt{m^2_1 + \Delta m^2_{sol}}$,

$$m_3 = \sqrt{m^2_1 + \Delta m^2_{sol} + \Delta m^2_{atm}} \qquad (40)$$

Inverted Hierarchy (IH) : $m_3 \ll m_1 < m_2$

Here, $m_3 = m_{\text{lightest}}$; $m_1 = \sqrt{m^2_3 + \Delta m^2_{atm}}$,

$$m_2 = \sqrt{m^2_3 + \Delta m^2_{atm} + \Delta m^2_{sol}} \qquad (41)$$

Using these randomly generated input parameters and oscillation data, variations of effective mass with the lightest neutrino mass is displayed in Fig. 10. For comparison, we have taken the current experimental limits on the half-life and the corresponding mass parameter for the isotopes ^{76}Ge and ^{136}Xe as follows,

From left-panel of Fig. 10 and using bounds from neutrinoless double beta decay experiments and cosmology, it is quite clear that the standard mechanism is not the only way to realize $0\nu\beta\beta$ and more importantly, NH and IH patterns are insensitive to current experimental bound while the quasi degenerate (QD) pattern is disfavoured from cosmological data from PLANCK1 and PLANCK2. In principle,

Fig. 9 Feynman diagrams contributing to neutrinoless double beta decay with $W^- - W^-$ mediation via the exchange of virtual light neutrinos ν (left panel), and the exchange of virtual eV scale sterile-like neutrinos N (right panel)
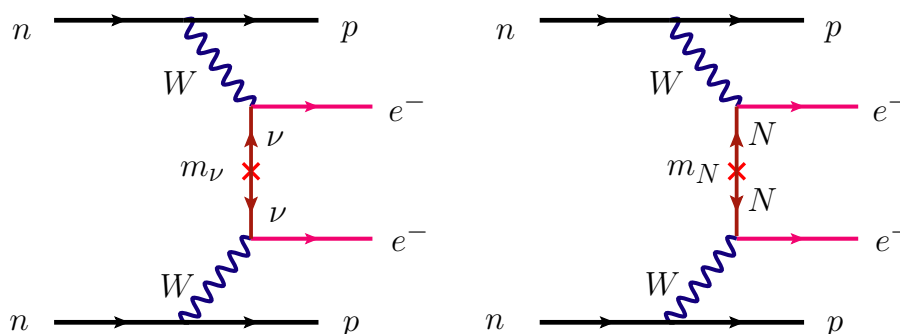
Table 6 The current lower limits on the half-life $T_{1/2}^{0\nu}$ and upper limits on the effective mass parameter $m_{\text{eff}}^{0\nu}$ of neutrinoless double beta decay for the isotopes ^{76}Ge and ^{136}Xe. The range for the effective mass parameter comes from different calculation methods for the nuclear matrix elements

Isotope	$T_{1/2}^{0\nu}$ [10^{25} yrs]	$m_{\text{eff}}^{0\nu}$ [eV]	Collaboration
^{76}Ge	> 2.1	< (0.2 − 0.4)	GERDA [94]
^{136}Xe	> 1.6	< (0.14 − 0.38)	EXO [95]
^{136}Xe	> 1.9	n/a	KamLAND-Zen [96]
^{136}Xe	> 3.6	< (0.12 − 0.25)	EXO + KamLAND-Zen combined [96]
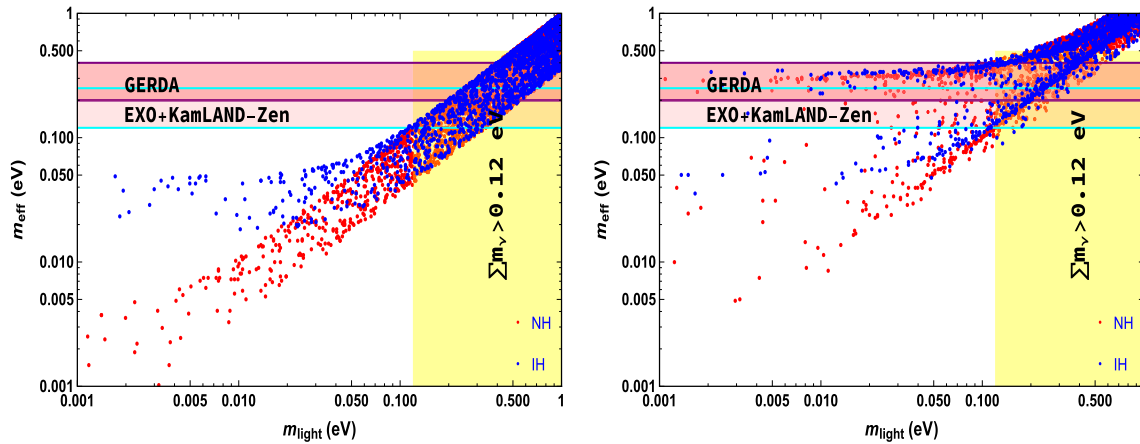
Fig. 10 Left Panel: Variation of effective Majorana mass as a function of the lightest neutrino mass, m_1 (m_3) for NH (IH) due to standard mechanism through light active Majoana neutrinos. Right Panel: The new physics contributions (in the presence of eV scale sterile-like neutrino, that falls in the experimental bound discussed in Table 6) to $0\nu\beta\beta$ vs lightest neutrino mass, m_1 (m_3) for NH (IH). The NH contributions are displayed by red dots band while the IH contributions are given by blue dots. The vertical shaded area is for constraint on the sum of light neutrino masses from recent cosmological data (PLANCK1 and PLANCK2). The horizontal shaded areas are for the limits in effective Majorana mass parameter and half-life by GERDA and EXO+KamLAND-Zen experiments

we should explore all possible sources of new physics that violate lepton number (effectively) by two units and can lead to $0\nu\beta\beta$.

We explicitly found that in addition to the standard mechanism, however, there is an additional contribution coming from the new eV scale sterile-like neutrino. In general the light (ν) and sterile-like (N) neutrino exchange can give the corresponding effective Majorana parameter as

$$m_{ee}^{\text{tot}} = m_{ee}^{\nu} + m_{ee}^{N} = \left(\sum_{i=1}^{3} U_{ei}^2 m_i + \sum_{i \in \text{eV}} U_{e4}^2 m_{si} \right), \quad (42)$$

where U_{e4} is the mixing between eV scale sterile neutrino with light active neutrino which has already expressed in terms of model parameters.

The variation of effective Majorana mass parameter in the presence of an additional eV scale sterile neutrino with the lightest neutrino mass is displayed in right-panel of Fig. 10. From this plot, we conclude that presence of an additional eV scale sterile-like neutrino enhances the predictability of the model by contributing to the NDBD (shown in Feynman

diagram in Fig. 9). The dotted points which lies in the horizontal bands shows that this new physics contribution can saturate the experimental bounds from GERDA and KAMLAND on effective neutrino mass [97,98] and can shed light on lepton number violation in nature along-with its implication to cosmology like matter-antimatter asymmetry of the universe.

5 Dark matter phenomenology

The model includes two heavy Majorana neutrinos N_2 and N_3 with exotic B − L charge −4, which ensures their stability by forbidding the interaction with SM particles, and the interaction Lagrangian is given as

$$\mathcal{L}_{\text{DM}} = \sum_{\alpha=2,3} i \overline{N_\alpha} \gamma^\mu D_\mu N_\alpha$$
$$- \sum_{\alpha,\beta=2,3} \left[y_{\alpha\beta} N_\alpha N_\beta \phi_8 + \text{H.c} \right], \quad (43)$$

Fig. 11 Annihilation channels for N_{D2} contributing to relic density and similar diagrams will be followed for N_{D3}
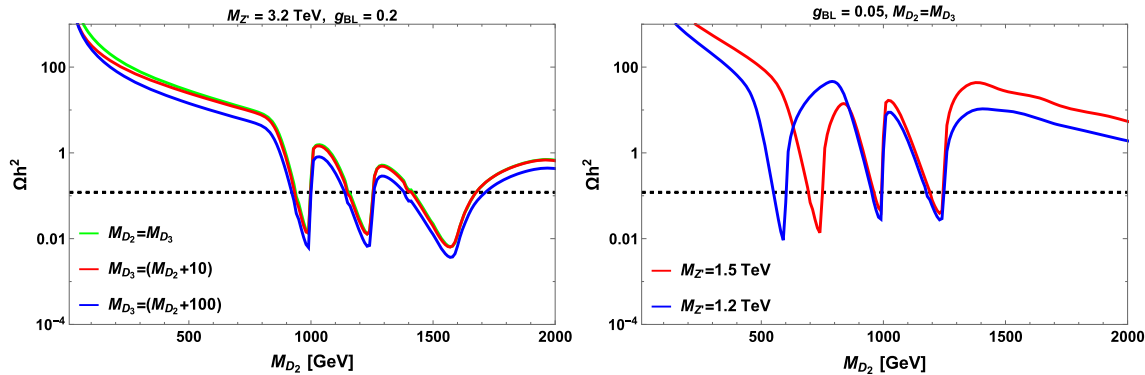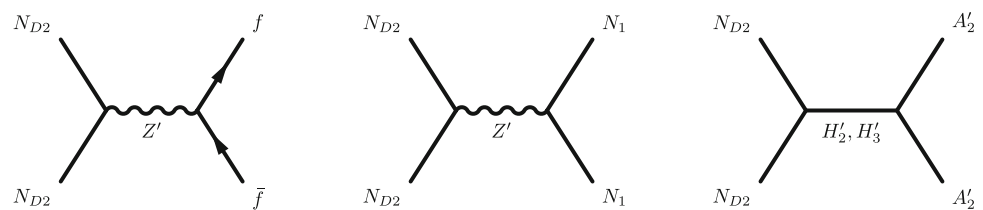
Fig. 12 Variation of relic density as a function of DM mass (M_{D_2}) with fixed Z' mass and g_{BL} for different set of mass splittings between M_{D_2} and M_{D_3}. Right panel corresponds to the behavior of relic density by varying Z' mass for $M_{D_2} = M_{D_3}$. The benchmark for the masses of

the scalars are $(M_{H'_1}, M_{H'_2}, M_{H'_3}, M_{A'_1}, M_{A'_2}) = (2.2, 2, 2.5, 2.1, 0.9)$ (in TeV). Horizontal dashed lines represent 3σ range of Planck limit on relic density

where $D_\mu = \partial_\mu - 4i g_{BL} Z'_\mu$. These fermions acquire masses when the local $B - L$ symmetry is broken and thereby leading to an inherent symmetry of $N_{2,3} \rightarrow -N_{2,3}$, which mimics the Z_2 symmetry, ensuring the stability of the DM [12,99]. All the two body decays of these DM candidates are kinematically forbidden at re-normalizable level, since all the generic Yukawa interactions with SM leptons are not allowed and by assuming the mass of the scalar field is greater than mass of the dark matter candidates. The mixing matrix of these two neutral fermions from (43) is given by

$$M_R = \begin{pmatrix} y_{22} \frac{v_8}{\sqrt{2}} & y_{23} \frac{v_8}{\sqrt{2}} \\ y_{23} \frac{v_8}{\sqrt{2}} & y_{33} \frac{v_8}{\sqrt{2}} \end{pmatrix}. \tag{44}$$

The above mass matrix can be diagonalized by orthogonal transformation:$U_R M_R U_R{}^T = M_D$, where

$$U_R = \begin{pmatrix} \cos\theta & \sin\theta \\ -\sin\theta & \cos\theta \end{pmatrix}, \qquad M_D = \begin{pmatrix} M_{D_2} & 0 \\ 0 & M_{D_3} \end{pmatrix}. \tag{45}$$

Here, the mixing angle is given by $\theta = \frac{1}{2} \tan^{-1} \left[\frac{2 y_{23} v_8}{y_{33} v_8 - y_{22} v_8} \right]$. The flavor and mass eigenstates are related by

$$N_2 = \cos\theta \, N_{D2} + \sin\theta \, N_{D3},$$
$$N_3 = -\sin\theta \, N_{D2} + \cos\theta \, N_{D3}. \tag{46}$$

In the present context, both of mass eigenstates N_{D2}, N_{D3} are stable dark matter candidates as both of them do not decay and hence, the total relic is summed up ($\Omega h^2 = \Omega_2 h^2 + \Omega_3 h^2$) [100]. Due to the same quantum numbers and similar mass mechanism, both of the heavy fermions will have comparable masses, but a small mass splitting can be generated by adjusting the Yukawa couplings. Using Eq. 46 in Eq. 43, one can show that the interference terms (involving N_{D2} and N_{D3}) with the gauge boson Z' and the scalar ϕ_8 vanishes. Hence, there will be no coannihilation effect in the computation of relic density. We use the well-known packages LanHEP [101] and micrOMEGAs [102–104] for the DM analysis. Channels giving significant contribution to relic density are shown in Fig. 11. Annihilation to sterile-like neutrinos ($N_1 N_1$ in final state) in gauge portal and CP-odd scalars ($A'_2 A'_2$ in final state) in scalar portal, stand out to give major contribution. We have fixed the masses of the scalar spectrum and gave emphasis to the impact of gauge parameters M'_Z and g_{BL} on relic density. Left panel of Fig. 12 depicts the behavior of relic density with DM mass (M_{D_2}) for various mass splittings between M_{D_2} and M_{D_3}, the right panel represents the behavior for different Z' masses. Relic density
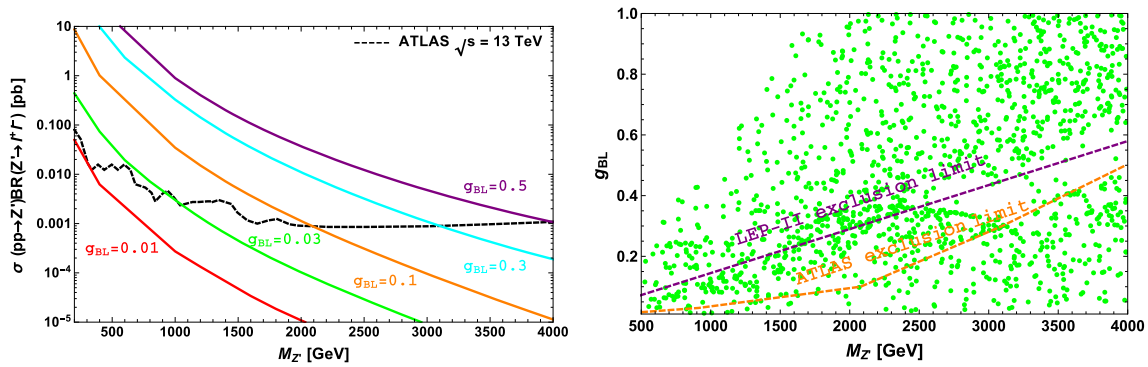
Fig. 13 Colored lines in left panel represent the dilepton signal cross section as a funciton of $M_{Z'}$ for different values of g_{BL} with the black dashed line points to ATLAS bound [105]. Right panel projects the constraint by ATLAS and LEP-II [106] on the gauge parameter space for $M_{D_2} = M_{D_3}$

with s-channel contribution is supposed to give resonance in the propagator (Z', H'_2, H'_4).

As Z' couples axial vectorially with DM fermion and vectorially with SM fermion, the WIMP-nucleon cross-section is not sensitive to direct detection experiments. Moving to the parameter scan, the gauge parameters $M_{Z'}$ and g_{BL} are restricted from the searches of dilepton signals in Z'-portal by ATLAS [105], and also LEP-II [106]. We have used CalcHEP [107,108] to obtain the cross section $pp \rightarrow Z' \rightarrow ee(\mu\mu)$ as a function Z' mass, depicted in the left panel of Fig. 13. It can be seen that for $g_{BL} = 0.01$, the region $M_{Z'} < 0.3$ TeV is excluded and for $g_{BL} = 0.03$, the allowed region is $M_{Z'} > 0.9$ TeV. For $g_{BL} = 0.1$, the $M_{Z'}$ should be above 2 TeV. $M_{Z'} > 3$ TeV is allowed for $g_{BL} = 0.3$ and heavy mass regime for Z' (above 4 TeV) is favorable for $g_{BL} = 0.5$. Right panel of Fig. 13 projects the parameter space consistent with Planck relic density limit upto 3σ range, with the exclusion limits of ATLAS and LEP-II $\left(\frac{M_{Z'}}{g_{BL}} > 6.9 \text{ TeV}\right)$. The favorable region refers to the data points below both the experimental bounds.

6 Summary and conclusion

In this article, we have presented a detail study of neutrino and dark matter phenomenology in a minimal extension of Standard Model with U(1)$_{B-L}$ and A_4 flavor symmetry. The model includes additional three neutral fermions with exotic $B - L$ charges of $-4, -4$ and 5 for cancellation of triangle gauge anomalies. The scalar sector is enriched with six SM singlet fields, of them, three are assigned with U(1)$_{B-L}$ charges and the rest three are charged under A_4 flavor symmetry. The former scalar fields helps in spontaneous breaking of $B - L$ symmetry and one massless mode of the CP odd eigenstates gets absorbed by the new gauge boson Z'. The later scalar fields, known as A_4 flavons, break the A_4 flavor symmetry spontaneously at high scale before the breaking of $U(1)_{B-L}$.

As different short-baseline experiments such as LSND, MiniBooNE etc. are pointing towards the existence of eV scale sterile neutrinos to explain certain experimental discrepancies, we tried to address the neutrino phenomenology with a fourth generation sterile-like neutrino. Out of the three exotic fermions in the model, one is in eV scale (sterile-like) and rest of them are in TeV scale, which help in explaining the neutrino mass and DM simultaneously. The presence of discrete symmetry provides a specific flavor structure to the neutrino mass matrix, leads to a better phenomenological consequences of neutrino mixing with a fourth generation sterile-like neutrino. We explored the active-sterile mixing in compatible with the current experimental observation. We found a large θ_{13} and associated non-zero CP phase, within the observed 3σ range of LSND data by introducing a perturbation term to the Lagrangian. Presence of eV scale sterile-like neutrino also provides an allowed parameter space for the effective neutrino mass in NDBD, lies within the experimental bound of KamLAND-Zen and GERDA. We strongly constrained the model parameters from the cosmological bound of active neutrino masses and showed the correlation between different mixing angles.

Apart from neutrino mixing, we studied the dark matter phenomenology with rest two exotic fermions, by generating the tree level mass in TeV scale unlike the eV scale sterile-like neutrino. By introducing suitable singlet scalar, the mass mechanism for these heavy fermions is assured by the $B - L$ breaking in TeV scale. Within the model framework, we found that both the Majorana fermions satisfy the correct DM relic density and the total contribution follows the 3σ observation of Planck, with s-channel annihilation processes in scalar and new gauge portal. As expected, the s-channel resonances for scalars and heavy gauge boson are obtained in the relic density, we have also analyzed the behavior for different values of model parameters. We also strongly constrained the parameters associated with gauge mediated processes from the ATLAS studies of di-lepton signals and LEP II. We have shown the allowed parameter space satis-

fying DM and collider constraints. Direct detection of dark matter in Z' portal is insensitive to direct detection experiments because of the Majorana nature. Finally, the proposed idea of extending SM with both gauge and flavor symmetries provides a suitable platform to investigate both neutrino and dark sectors.

Data Availability Statement This manuscript has no associated data or the data will not be deposited. [Authors' comment: All the data relevant to this publication are available in the text and in graphical form through the plots.]

Appendix

A_4 symmetry includes three and one dimensional irreducible representations.
If (a_1, a_2, a_3) and (b_1, b_2, b_3) are the triplets of A_4, tensor products of these triplets are given as following

$$3 \otimes 3 = 3_s \oplus 3_A \oplus 1 \oplus 1' \oplus 1'',$$
$$1 \otimes 1 = 1, \quad 1' \otimes 1'' = 1,$$
$$1' \otimes 1' = 1'', \quad 1'' \otimes 1'' = 1',$$

$$\text{where} \quad 3_s = \begin{pmatrix} 2a_1b_1 - a_2b_3 - a_3b_2 \\ 2a_3b_3 - a_1b_2 - b_1a_2 \\ 2a_2b_2 - a_3b_1 - a_1b_3 \end{pmatrix},$$

$$3_A = \begin{pmatrix} a_2b_3 - a_3b_2 \\ a_1b_2 - a_2b_1 \\ a_3b_1 - a_1b_3 \end{pmatrix},$$

$$1 = a_1b_1 + a_2b_3 + a_3b_2,$$
$$1' = a_3b_3 + a_1b_2 + a_2b_1,$$
$$1'' = a_2b_2 + a_3b_1 + a_1b_3.$$

References

1. R.N. Mohapatra, G. Senjanovic, Phys. Rev. Lett. **44**, 912 (1980). [231(1979)]
2. S.M. Barr, Phys. Rev. Lett. **92**, 101601 (2004). arXiv:hep-ph/0309152 [hep-ph]
3. E.K. Akhmedov, M. Frigerio, JHEP **01**, 043 (2007). arXiv:hep-ph/0609046 [hep-ph]
4. E.K. Akhmedov, Nucl. Phys. Proc. Suppl. **87**, 321 (2000). [321(1999)], arXiv:hep-ph/0001041 [hep-ph]
5. Y. Cai, J. Herrero-García, M.A. Schmidt, A. Vicente, R.R. Volkas, Front. Phys. **5**, 63 (2017). arXiv:1706.08524
6. O.G. Miranda, J.W.F. Valle, Nucl. Phys. B **908**, 436 (2016). arXiv:1602.00864
7. O.L.G. Peres, A.Y. Smirnov, Nucl. Phys. B **599**, 3 (2001). arXiv:hep-ph/0011054 [hep-ph]
8. M. Sorel, J.M. Conrad, M. Shaevitz, Phys. Rev. D **70**, 073004 (2004). arXiv:hep-ph/0305255 [hep-ph]
9. S. Vagnozzi, E. Giusarma, O. Mena, K. Freese, M. Gerbino, S. Ho, M. Lattanzi, Phys. Rev. D **96**, 123503 (2017). arXiv:1701.08172
10. J. Kopp, M. Maltoni, T. Schwetz, Phys. Rev. Lett. **107**, 091801 (2011). arXiv:1103.4570
11. C. Giunti, M. Laveder, Phys. Rev. D **84**, 073008 (2011). arXiv:1107.1452
12. C. Bonilla, S. Centelles-Chuliá, R. Cepedello, E. Peinado, R. Srivastava (2018). arXiv:1812.01599
13. J. Heeck, W. Rodejohann, Phys. Rev. D **87**, 037301 (2013). arXiv:1211.5295
14. A. Aguilar-Arevalo et al., (LSND) Phys. Rev. D **64**, 112007 (2001). arXiv:hep-ex/0104049 [hep-ex]
15. M. Tanabashi et al., (Particle Data Group), Phys. Rev. D **98**, 030001 (2018)
16. N. Aghanim et al. (Planck) (2018). arXiv:1807.06209
17. C. Blanco, D. Hooper, P. Machado (2019). arXiv:1901.08094
18. A.A. Aguilar-Arevalo et al., (MiniBooNE) Phys. Rev. Lett. **110**, 161801 (2013). arXiv:1303.2588
19. M. Dentler, í. Hernández-Cabezudo, J. Kopp, P. A. N. Machado, M. Maltoni, I. Martinez-Soler, T. Schwetz, JHEP **08**, 010 (2018). arXiv:1803.10661
20. J. Barry, W. Rodejohann, H. Zhang, JHEP **07**, 091 (2011). arXiv:1105.3911
21. A. Merle, V. Niro, JCAP **1107**, 023 (2011). arXiv:1105.5136
22. H. Zhang, Phys. Lett. B **714**, 262 (2012). arXiv:1110.6838
23. P.S. Bhupal Dev, A. Pilaftsis, Phys. Rev. **D87**, 053007 (2013). arXiv:1212.3808
24. Y. Zhang, X. Ji, R.N. Mohapatra, JHEP **10**, 104 (2013). arXiv:1307.6178
25. A. Das, T. Nomura, H. Okada, S. Roy, Phys. Rev. D **96**, 075001 (2017). arXiv:1704.02078
26. A. Das, P.S.B. Dev, N. Okada, Phys. Lett. B **799**, 135052 (2019a). arXiv:1906.04132
27. M. Frank, L. Selbuz, Phys. Rev. D **88**, 055003 (2013). arXiv:1308.5243
28. R. Adhikari, D. Borah, E. Ma, Phys. Lett. B **755**, 414 (2016). arXiv:1512.05491
29. N. Nath, M. Ghosh, S. Goswami, S. Gupta, JHEP **03**, 075 (2017). arXiv:1610.09090
30. P. Das, A. Mukherjee, M.K. Das, Nucl. Phys. B **941**, 755 (2019b). arXiv:1805.09231
31. S. Gariazzo, P. de Salas, S. Pastor, JCAP **07**, 014 (2019). arXiv:1905.11290
32. C.S. Pires, Phys. Lett. B **800**, 135135 (2020). arXiv:1908.09313
33. S. Hannestad, R.S. Hansen, T. Tram, Phys. Rev. Lett. **112**, 031802 (2014). arXiv:1310.5926

34. M. Archidiacono, S. Hannestad, R.S. Hansen, T. Tram, Phys. Rev. D **93**, 045004 (2016). arXiv:1508.02504

35. B. Dasgupta, J. Kopp, Phys. Rev. Lett. **112**, 031803 (2014). arXiv:1310.6337

36. S. Hannestad, I. Tamborra, T. Tram, JCAP **07**, 025 (2012). arXiv:1204.5861

37. D.S. Akerib et al., (LUX) Phys. Rev. Lett. **112**, 091303 (2014). arXiv:1310.8214

38. E. Aprile et al., (XENON100) Phys. Rev. Lett. **109**, 181301 (2012). arXiv:1207.5988

39. M.G. Aartsen et al., (IceCube) Phys. Rev. Lett. **110**, 131302 (2013). arxiv:1212.4097

40. M. Ackermann et al., (Fermi-LAT) Phys. Rev. D **88**, 082002 (2013). arXiv:1305.5597

41. M. Aguilar et al., (AMS) Phys. Rev. Lett. **110**, 141102 (2013)

42. A. Abramowski et al., (H.E.S.S.) Phys. Rev. Lett. **110**, 041301 (2013). arXiv:1301.1173

43. J. Aleksić et al., JCAP **1402**, 008 (2014). arXiv:1312.1535

44. S.T. Petcov, A.V. Titov, Int. J. Mod. Phys. A **33**, 1844024 (2018a)

45. E. Ma, G. Rajasekaran, Phys. Rev. D **64**, 113012 (2001). arXiv:hep-ph/0106291 [hep-ph]

46. G. Altarelli, F. Feruglio, Nucl. Phys. B **741**, 215 (2006). arXiv:hep-ph/0512103 [hep-ph]

47. G. Altarelli, D. Meloni, J. Phys. **G36**, 085005 (2009). arXiv:0905.0620

48. S.T. Petcov, A.V. Titov, Phys. Rev. D **97**, 115045 (2018b). arXiv:1804.00182

49. E. Ma, A. Natale, A. Rashed, Int. J. Mod. Phys. A **27**, 1250134 (2012). arXiv:1206.1570

50. S.F. King, C. Luhn, Rept. Prog. Phys. **76**, 056201 (2013). arXiv:1301.1340

51. M.S. Boucenna, M. Hirsch, S. Morisi, E. Peinado, M. Taoso, J.W.F. Valle, JHEP **05**, 037 (2011). arXiv:1101.2874

52. D. Meloni, S. Morisi, E. Peinado, Phys. Lett. B **697**, 339 (2011). arXiv:1011.1371

53. A. Mukherjee, M.K. Das, Nucl. Phys. B **913**, 643 (2016). arXiv:1512.02384

54. S. Bhattacharya, B. Karmakar, N. Sahu, A. Sil, Phys. Rev. D **93**, 115041 (2016). arXiv:1603.04776

55. L.M.G. De La Vega, R. Ferro-Hernandez, E. Peinado, Phys. Rev. D **99**, 055044 (2019). arXiv:1811.10619

56. R.N. Mohapatra, J.C. Pati, Phys. Rev. D **11**, 2558 (1975)

57. J. C. Pati, A. Salam, Phys. Rev. D **10**, 275 (1974). [Erratum: Phys. Rev.D11,703(1975)]

58. G. Senjanovic, R.N. Mohapatra, Phys. Rev. D **12**, 1502 (1975)

59. G. Senjanovic, Nucl. Phys. B **153**, 334 (1979)

60. R.N. Mohapatra, G. Senjanovic, Phys. Rev. D **23**, 165 (1981)

61. J. Heeck, S. Patra, Phys. Rev. Lett. **115**, 121804 (2015). arXiv:1507.01584

62. J.C. Montero, V. Pleitez, Phys. Lett. B **675**, 64 (2009). arXiv:0706.0473

63. E. Ma, R. Srivastava, Phys. Lett. B **741**, 217 (2015a). arXiv:1411.5042

64. E. Ma, R. Srivastava, Mod. Phys. Lett. A **30**, 1530020 (2015b). arXiv:1504.00111

65. S. Singirala, R. Mohanta, S. Patra (2017). arXiv:1704.01107

66. S. Singirala, R. Mohanta, S. Patra, S. Rao, JCAP **1811**, 026 (2018). arXiv:1710.05775

67. C.-Q. Geng, H. Okada, Phys. Dark Univ. **20**, 13 (2018). arXiv:1710.09536

68. T. Nomura, H. Okada, Eur. Phys. J. **C78**, 189 (2018a). arXiv:1708.08737

69. T. Nomura, H. Okada, Nucl. Phys. B **941**, 586 (2019). arXiv:1705.08309

70. T. Nomura, H. Okada, Phys. Lett. B **781**, 561 (2018b). arXiv:1711.05115

71. T. Kobayashi, Y. Omura, K. Yoshioka, Phys. Rev. D **78**, 115006 (2008). arXiv:0809.3064

72. S.F. King, C. Luhn, JHEP **09**, 042 (2011). arXiv:1107.5332

73. G. Altarelli, F. Feruglio, Nucl. Phys. B **720**, 64 (2005). arXiv:hep-ph/0504165 [hep-ph]

74. F. Feruglio, C. Hagedorn, L. Merlo, JHEP **03**, 084 (2010). arXiv:0910.4058

75. D. Borah, M.K. Das, A. Mukherjee, Phys. Rev. D **97**, 115009 (2018). arXiv:1711.02445

76. E. Ma, Mod. Phys. Lett. A **25**, 2215 (2010). arXiv:0908.3165

77. N. Memenga, W. Rodejohann, H. Zhang, Phys. Rev. D **87**, 053021 (2013). arXiv:1301.2963

78. D. Meloni, Front.in Phys. **5**, 43 (2017). arXiv:1709.02662

79. K.S. Channey, S. Kumar, J. Phys. **G46**, 015001 (2019). arXiv:1812.10268

80. S.K. Garg, Nucl. Phys. B **931**, 469 (2018). arXiv:1712.02212

81. S. Dev, D. Raj, R.R. Gautam, Nucl. Phys. B **911**, 744 (2016). arXiv:1607.08051

82. S. Dev, S. Gupta, R.R. Gautam, Mod. Phys. Lett. A **26**, 501 (2011). arXiv:1011.5587

83. P.F. de Salas, D.V. Forero, C.A. Ternes, M. Tortola, J.W.F. Valle, Phys. Lett. B **782**, 633 (2018). arXiv:1708.01186

84. S. Gariazzo, M. Archidiacono, P.F. de Salas, O. Mena, C.A. Ternes, M. Tórtola, JCAP **1803**, 011 (2018). arXiv:1801.04946

85. C. Giunti, E.M. Zavanin, JHEP **07**, 171 (2015). arXiv:1505.00978

86. A. Abada, í. Hernández-Cabezudo, X. Marcano, JHEP **01**, 041 (2019). arXiv:1807.01331

87. C. Giunti, T. Lasserre (2019). arXiv:1901.08330

88. G.-Y. Huang, S. Zhou, Nucl. Phys. B **945**, 114691 (2019). arXiv:1902.03839

89. A. Nucciotti, eConf **C070512**, 025 (2007). arXiv:0707.2216

90. R. G. H. Robertson (KATRIN). In: Proceedings, 2013 Community Summer Study on the Future of U.S. Particle Physics: Snowmass on the Mississippi (CSS2013): Minneapolis, MN, USA, July 29-August 6, 2013 (2013). arXiv:1307.5486, http://www.slac.stanford.edu/econf/C1307292/docs/submittedArxivFiles/1307.5486.pdf

91. L. Cardani, Sci. Post Phys. Proc. **1**, 024 (2019). arxiv:1810.12828

92. M. J. Dolinski, A. W. P. Poon, W. Rodejohann (2019). arXiv:1902.04097

93. R. Henning, Rev. Phys. **1**, 29 (2016)

94. M. Agostini et al., (GERDA) Phys. Rev. Lett. **111**, 122503 (2013). arXiv:1307.4720

95. M. Auger et al., (EXO-200) Phys. Rev. Lett. **109**, 032505 (2012). arXiv:1205.5608

96. A. Gando et al., (KamLAND-Zen) Phys. Rev. Lett. **110**, 062502 (2013). arXiv:1211.3863

97. P.F. De Salas, S. Gariazzo, O. Mena, C.A. Ternes, M. Tórtola, Front. Astron. Space Sci. **5**, 36 (2018). arXiv:1806.11051

98. J.T. Penedo, S.T. Petcov, Phys. Lett. B **786**, 410 (2018). arXiv:1806.03203

99. C. Bonilla, E. Peinado, R. Srivastava, LHEP **2**, 124 (2019). arXiv:1903.01477

100. N. Bernal, D. Restrepo, C. Yaguna, í. Zapata, Phys. Rev. D **99**, 015038 (2019). arXiv:1808.03352

101. A. V. Semenov (1996). arXiv:hep-ph/9608488 [hep-ph]

102. A. Pukhov, E. Boos, M. Dubinin, V. Edneral, V. Ilyin, D. Kovalenko, A. Kryukov, V. Savrin, S. Shichanin, A. Semenov (1999). arXiv:hep-ph/9908288 [hep-ph]

103. G. Belanger, F. Boudjema, A. Pukhov, A. Semenov, Comput. Phys. Commun. **176**, 367 (2007). arXiv:hep-ph/0607059 [hep-ph]

104. G. Belanger, F. Boudjema, A. Pukhov, A. Semenov, Comput. Phys. Commun. **180**, 747 (2009). arXiv:0803.2360

105. Tech. Rep. ATLAS-CONF-2015-070, CERN, Geneva (2015). https://cds.cern.ch/record/2114842

106. S. Schael et al., (DELPHI, OPAL, LEP Electroweak, ALEPH, L3) Phys. Rept. **532**, 119 (2013). arXiv:1302.3415
107. A. Belyaev, N.D. Christensen, A. Pukhov, Comput. Phys. Commun. **184**, 1729 (2013). arXiv:1207.6082
108. K. Kong, In: The Dark Secrets of the Terascale: Proceedings, TASI 2011, Boulder, Colorado, USA, Jun 6 - Jul 11, 2011 (2013), pp. 161–198. arXiv:1208.0035, https://inspirehep.net/record/1124593/files/arXiv:1208.0035.pdf